Robotica (2011) volume 29, pp. 585–593. © Cambridge University Press 2010
doi:10.1017/S0263574710000342

An optimization method for the reference trajectory of parametric excitation walking

Kouichi Taji†*, Yoshihisa Banno† and Yuji Harata‡

†*Department of Mechanical Science and Engineering, Graduate School of Engineering, Nagoya University, Furocho, Chikusa, Nagoya 464-8603, Japan. E-mail: y_banno@nuem.nagoya-u.ac.jp*
‡*Division of Mechanical Systems and Applied Mechanics, Faculty of Engineering, Hiroshima University, 1-4-1, Kagamiyama, Higashi-Hiroshima, Japan. E-mail: harata@hiroshima-u.ac.jp*

(Received in Final Form: July 16, 2010. First published online: August 18, 2010)

SUMMARY
In parametric excitation walking, up-and-down motion of the center of mass restores mechanical energy and sustainable gait is generated. Not only walking performance but also walking ability strongly depends on the reference trajectory of the center of mass. In this paper, we propose an optimization method for the reference trajectory, in which the reference trajectory is confined to the quartic spline curves and the parameters of spline curves are optimized by a local search method usually used in combinatorial optimization. We apply the proposed method to a kneed biped robot and find some remarkably interesting results by numerical simulations.

KEYWORDS: Bipeds; Legged robots; Parametric excitation; Optimization; Dynamic walking.

1. Introduction

Parametric excitation is a method to increase mechanical energy of a system by up-and-down movement of the center of mass (CoM). A children's swing is an example using parametric excitation principle. Parametric excitation walking was first proposed by Asano *et al.*[1] They applied the parametric excitation principle to the biped robot with telescopic legs and showed that the robot walked sustainably by making CoM of swing leg up-and-down by telescopic mechanism. Harata *et al.*[2,3] applied the parametric excitation method to a kneed biped robot, in which the up-and-down motion of the CoM was realized by bending and stretching a knee, and showed that sustainable gait was generated by knee torque only. Harata *et al.*[4,5] also proposed parametric excitation-based inverse bending walking in which a swing-leg knee was bent in the inverse direction to human.

The most important thing to apply the parametric excitation principle is to move CoM along an appropriate trajectory. For a pendulum, Lavrovskii and Formal'skii[6] proved the optimal trajectory, A→B→C→D→E, shown in Fig. 1, along which the increase of total mechanical energy was maximized, supposed that the length of a pendulum l was changed instantaneously. The optimal trajectory shown in Fig. 1 has nothing but theoretical meaning because CoM cannot be moved instantaneously in real machines. Moreover, there is a significant difference between a pendulum and a biped robot in that the hip joint of a biped robot is movable while the supporting point of a pendulum is fixed at a ceiling and, hence, the trajectory of Fig. 1 may not be optimal for biped robots.

In spite of this, Asano *et al.*[1] adopted the smoothing approximate reference trajectory of that depicted in Fig. 1 by using the cubic sinusoid, and realized sustainable walking on a level ground. Harata *et al.*[2,3] also used the cubic sinusoid for the reference trajectory of the swing-leg knee angle.

In this paper, we propose an optimization method for the reference trajectory of the kneed biped robot proposed by Harata *et al.*[2,3] In this model, knee torque is designed to track completely a reference trajectory for the knee angle of swing leg. Hence, not only walking performance but also walking possibility strongly depends on the reference trajectory. For a biped robot, Chevallereau and Aoustin[7] proposed an optimization method for reference trajectories. In their method, a reference trajectory is limited as quartic spline curves, and their coefficients are treated as decision variables, and then, general nonlinear optimization solver is used to optimize these coefficients.

The proposed method also uses quartic spline curves for a reference trajectory, and their coefficients are optimized. Both the models of ref. [7] and this paper deal with under-actuated system, but there is a significant difference between the biped model in this paper and that of ref. [7]. Our model has 3 degrees of freedom with only one actuator at a swing-leg knee while the model of ref. [7] has 5 degrees of freedom with four actuators. Thus, by taking into account physical constraints such as the momentum conservation law and a reaction force from the ground, Chevallereau and Aoustin's[7] model can be dealt with as if a full-actuated system. In contrast to this, our model cannot be treated as a full-actuated system, because the stance at heel strike cannot be determined *a priori* and, hence, it must rely on numerical simulation.

Therefore, the proposed optimization method adopts the following strategy. We first generate a steady gait for a certain (already known) reference trajectory and then generate a steady gait for a slightly perturbed trajectory. To do this, we discretize the search space for parameters and utilize a local search method usually used in combinational optimization problems.

* Corresponding author. E-mail: taji@nuem.nagoya-u.ac.jp

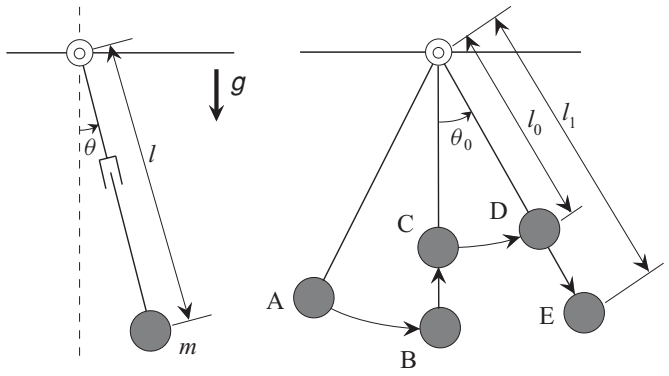

Fig. 1. Optimal trajectory of the pendulum for parametric excitation.

To show the practical efficiency of the proposed method, we apply the method to optimize the reference trajectory of the relative knee angle of the kneed biped robot.[2,3] The numerical experiments show that the trajectories constructed by quartic spline are more flexible and more efficient than those by cubic sinusoid used in the previous papers.[2,3] Moreover, the optimal trajectory shown in Fig. 1 for a pendulum is proven to be almost optimal for the biped robot from a viewpoint of walking speed.

This paper is organized as follows. Section 2 explains the model of a biped robot treated in this paper and parametric excitation walking. In Section 3, we first introduce the reference trajectory using the quartic spline curve and then propose the optimization method for the reference trajectory. Section 4 shows the numerical results of the proposed method. Finally, in Section 5, we conclude.

2. Parametric Excitation Walking

In this section, we first introduce the biped robot treated in this paper and then explain the parametric excitation walking proposed by Harata *et al.*[2,3] For details, please refer to ref. [3].

2.1. Model of planar biped robot with semicircular feet

Figure 2 illustrates the model of a biped robot treated in this paper. The robot has five point masses, such that each leg has two masses and the remaining one is at the hip joint, and has semicircular feet whose centers are on each leg. Each leg has an actuated knee joint, but the support leg is fixed in a straight posture (see Fig. 2). Therefore, the robot has 3 degrees of freedom, and the three angles θ_1, θ_2, and θ_3 shown in Fig. 2 are taken as generalized coordinates. Each angle is taken in a clockwise direction from vertical upward.

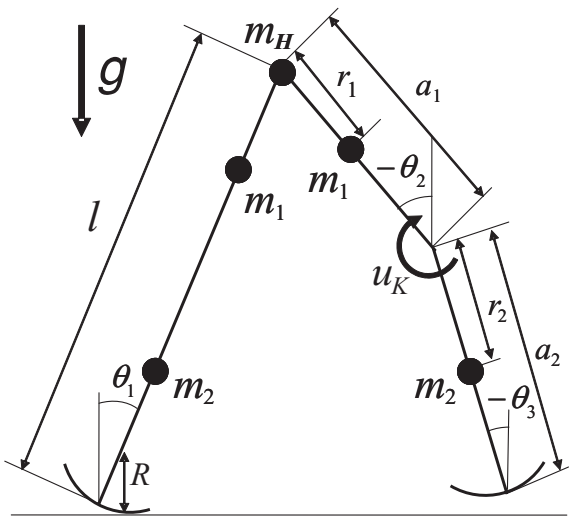

Fig. 2. Model of a planar kneed biped robot with semicircular feet.

In this model, the robot gait consists of the following three phases:

- The first phase (single support phase I): A support leg rotates around the contact point between a semicircular foot and the ground, and the knee of the swing leg is not fixed and, hence, the knee angle of the swing leg can be controlled by an input torque.
- The second phase (single support phase II): A support leg rotates around the contact point like phase I, but the swing-leg knee is fixed in a straight posture. When it turns from the first phase to the second phase, a completely inelastic collision is assumed to occur at the swing-leg knee.
- The third phase (double support phase): This phase occurs instantaneously when a swing leg touches down the ground, and then the role of a support leg and that of a swing leg are exchanged.

The dynamic equation during the single support phase takes the form

$$\boldsymbol{M}(\boldsymbol{\theta})\ddot{\boldsymbol{\theta}} + \boldsymbol{C}(\boldsymbol{\theta}, \dot{\boldsymbol{\theta}})\dot{\boldsymbol{\theta}} + \boldsymbol{g}(\boldsymbol{\theta}) = \boldsymbol{S}u_K - \boldsymbol{J}^{\mathrm{T}}\lambda, \tag{1}$$

where $\boldsymbol{\theta} = [\,\theta_1\ \theta_2\ \theta_3\,]^{\mathrm{T}}$ is the generalized coordinate vector, $\boldsymbol{M}$ is the inertia matrix, $\boldsymbol{C}$ is the Coriolis force and the centrifugal force, and $\boldsymbol{g}$ is the gravity vector. The matrix $\boldsymbol{J} = [\,0\ 1\ -1\,]$ is the Jacobian derived from the knee constraint, $\theta_2 = \theta_3$, and $\lambda \in \mathbb{R}$ is the knee binding force. The control input vector $\boldsymbol{S}u_K$ in Eq. (1) is given by

$$\boldsymbol{S}u_K = \begin{bmatrix} 0 \\ -1 \\ 1 \end{bmatrix} u_K, \tag{2}$$

where u_K is the input torque for a swing-leg knee.

We now explain impact equations. In the biped robot model dealt with in this paper, there are collisions at the knee and the ground. First, we explain an impact equation at the knee. When a swing leg straightens, a completely inelastic collision is assumed to occur at the knee of the swing leg. The coordinates $\dot{\boldsymbol{\theta}}^-$ and $\dot{\boldsymbol{\theta}}^+$, which correspond to before and after the knee impact, respectively, are related by the following equation:

$$\boldsymbol{M}(\boldsymbol{\theta})\dot{\boldsymbol{\theta}}^+ = \boldsymbol{M}(\boldsymbol{\theta})\dot{\boldsymbol{\theta}}^- + \boldsymbol{J}^T\lambda_K, \tag{3}$$

where λ_K is the constraint force making $\boldsymbol{J}\dot{\theta}^+ = 0$. This force is given by

$$\lambda_K = -(\boldsymbol{J}\boldsymbol{M}\,(\boldsymbol{\theta})^{-1}\,\boldsymbol{J}^T)^{-1}\boldsymbol{J}\dot{\boldsymbol{\theta}}^-. \tag{4}$$

From Eqs. (3) and (4), angular velocities after the knee impact are

$$\dot{\boldsymbol{\theta}}^+ = (\boldsymbol{I}_3 - \boldsymbol{M}(\boldsymbol{\theta})^{-1}\boldsymbol{J}^{\mathrm{T}}(\boldsymbol{J}\boldsymbol{M}(\boldsymbol{\theta})^{-1}\boldsymbol{J}^T)^{-1}\boldsymbol{J})\dot{\boldsymbol{\theta}}^-. \tag{5}$$

https://doi.org/10.1017/S0263574710000342 Published online by Cambridge University Press

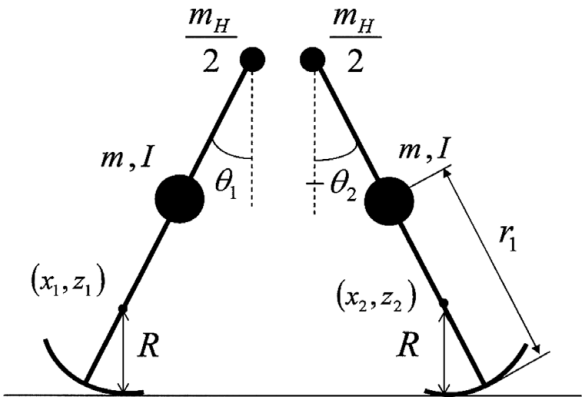

Fig. 3. Geometric relation at the heel-strike instant.

Angular positions do not change before and after the impact. We remark that, by using the control input explained below, a collision at a swing-leg knee just before phase II is negligible. Next, we explain the impact equation at the ground. We assume that a collision at the ground is completely inelastic. To derive the impact equation, we introduce the separated model shown by Fig. 3 and introduce the generalized coordinate of legs $i, (i = 1, 2)$, such as $\boldsymbol{q} = [\, q_1 \; q_2 \,]^{\mathrm{T}}$, where $\boldsymbol{q}_i = [\, x_i \; y_i \; \theta_i \,]^{\mathrm{T}}$. Let the superscripts "$-$" and "$+$" correspond to before and after the impact at the ground, respectively. Then, we have $\boldsymbol{q}^- = \boldsymbol{q}^+$, because the positions do not change before and after the impact. The impact equation of generalized coordinates takes the form

$$\bar{\boldsymbol{M}}\,(\boldsymbol{q})\,\dot{\boldsymbol{q}}^+ = \bar{\boldsymbol{M}}\,(\boldsymbol{q})\,\dot{\boldsymbol{q}}^- + \boldsymbol{J}_I\,(\boldsymbol{q})^{\mathrm{T}}\,\boldsymbol{\lambda}_I, \tag{6}$$

where $\boldsymbol{\lambda}_I$ is an undetermined multiplier vector corresponding to impulse force, such that $\boldsymbol{J}_I\,(\boldsymbol{q})\,\dot{\boldsymbol{q}}^+ = \boldsymbol{0}$, and $\bar{\boldsymbol{M}}(\boldsymbol{q}) \in \mathbb{R}^{6\times 6}$ is the inertia matrix.

There are some constraints among coordinates. First, from geometric conditions we have

$$\begin{aligned} z_2 &= R, \\ x_1 + (l-R)\sin\theta_1 &= x_2 + (l-R)\sin\theta_2, \\ z_1 + (l-R)\cos\theta_1 &= z_2 + (l-R)\cos\theta_2. \end{aligned} \tag{7}$$

These equations mean that the height of the center of foot of the support leg equals the foot radius, and that vertical and horizontal hip positions from (x_1, z_1) equal hip positions from (x_2, z_2). In addition, the rate constraint that the foot of the support leg rolls on the ground is given by

$$\dot{x}_2^+ = R\dot{\theta}_2^+. \tag{8}$$

The Jacobian $\boldsymbol{J}_I$ is derived by differentiating (7) and by incorporating (8), such that

$$\boldsymbol{J}_I = \begin{bmatrix} 0 & 0 & 0 & 0 & 1 & 0 \\ 1 & 0 & (l-R)\cos\theta_1 & -1 & 0 & -(l-R)\cos\theta_2 \\ 0 & 1 & -(l-R)\sin\theta_1 & 0 & -1 & (l-R)\sin\theta_2 \\ 0 & 0 & 0 & 1 & 0 & -R \end{bmatrix}. \tag{9}$$

The multiplier vector $\boldsymbol{\lambda}_I$ is given by

$$\boldsymbol{\lambda}_I = \left(\boldsymbol{J}_I \bar{\boldsymbol{M}}\,(\boldsymbol{q})^{-1}\,\boldsymbol{J}_I^T\right)^{-1}\boldsymbol{J}_I\dot{\boldsymbol{q}}^-. \tag{10}$$

Therefore, the velocity of the generalized coordinate after collision becomes

$$\dot{\boldsymbol{q}}^+ = \left(\boldsymbol{I}_6 - \bar{\boldsymbol{M}}(\boldsymbol{q})^{-1}\boldsymbol{J}_I^{\mathrm{T}}\left(\boldsymbol{J}_I\bar{\boldsymbol{M}}(\boldsymbol{q})^{-1}\boldsymbol{J}_I^T\right)^{-1}\boldsymbol{J}_I\right)\dot{\boldsymbol{q}}^-. \tag{11}$$

The dynamics of our biped robot is completely determined by the dynamic Eq. (1) and impact Eqs. (5) and (11).

2.2. Parametric excitation walking

In this subsection, we explain the application of the parametric excitation walking[2,3] to the robot introduced in the previous subsection. The reference trajectory $\tilde{h}$ of the relative angle of a swing leg is given in refs. [2,3] as follows:

$$\begin{aligned} \tilde{h}(t) &= (\theta_2(t) - \theta_3(t))_d \\ &= \begin{cases} A_m \sin^3\left(\dfrac{\pi}{T_{\mathrm{set}} - \delta}(t-\delta)\right) & (\delta \le t \le T_{\mathrm{set}}) \\ 0 & (\text{otherwise}), \end{cases} \end{aligned} \tag{12}$$

where A_m is the maximum bending angle, $\delta > 0$ is the beginning time of bending. The time parameter t means a relative time from the beginning of the first phase, that is, t is reset to be zero just after the third phase and T_{set} is the time just before the second phase. Therefore, the parameter T_{set} should be determined to be shorter than the walking period.

We remark that, by using the partial linearization method,[2,3] the input torque u_K for a swing-leg knee can be designed so that the relative knee angle completely coincides with a given reference trajectory, suppose that the trajectory is sufficiently smooth (e.g. the second derivative is continuous). For a reference trajectory of (12), the input torque is designed as

$$\begin{aligned} u_K = ([\,0 \quad 1 \quad -1\,]\boldsymbol{M}^{-1}\boldsymbol{S})^{-1}[\,0 \quad 1 \quad -1\,]\boldsymbol{M}^{-1} \\ \times(\boldsymbol{M}[\,0 \quad 0 \quad -\ddot{\tilde{h}}\,] + \boldsymbol{C}\dot{\boldsymbol{\theta}} + \boldsymbol{g}). \end{aligned} \tag{13}$$

3. Optimization Method for Reference Trajectories

In this section, we first introduce the reference trajectory using quartic spline curves and then propose an optimization method for a reference trajectory.

3.1. Reference trajectory using quartic spline curve

A quartic spline curve is given by

$$s(t) = a + bt + ct^2 + dt^3 + et^4. \tag{14}$$

Here, $a, b, c, d,$ and e are constant parameters, which are determined uniquely by five constraints. Let the time parameter t indicate a relative time from the beginning of the first phase, and T_{set} denote the time just before the second phase. Then, by using quartic spline curves, a reference trajectory for the relative knee angle $\theta_2 - \theta_3$ of the swing leg is designed during the first phase $[0, T_{set}]$. We first divide the time interval $[0, T_{set}]$ into seven intervals by

https://doi.org/10.1017/S0263574710000342 Published online by Cambridge University Press

six time parameters, $0 \le t_1 < t_2 < t_3 \le t_4 < t_5 < t_6 = T_{set}$, where t_1 denotes the beginning of bending, t_3 denotes the end of bending, t_4 denotes the beginning of stretching, and t_6 denotes the end of stretching. The remaining time parameters, t_2 and t_5, are additional points used to make a trajectory flexible and smooth. Thus, a swing-leg knee is kept in a straight posture during the interval $[0, t_1]$ and is maintained to be the maximum bending angle A_m during the interval $[t_3, t_4]$. Quartic spline curves should be designed for the four intervals: $[t_1, t_2]$, $[t_2, t_3]$, $[t_4, t_5]$, and $[t_5, t_6]$. Consequently, the reference trajectory h is given by

$$h_T(t) = (\theta_2(t) - \theta_3(t))_d = \begin{cases} 0 & \text{if } 0 \le t < t_1 \\ a_1 + b_1 t + c_1 t^2 + d_1 t^3 + e_1 t^4 & \text{if } t_1 \le t \le t_2 \\ a_2 + b_2 t + c_2 t^2 + d_2 t^3 + e_2 t^4 & \text{if } t_2 \le t \le t_3 \\ A_m & \text{if } t_3 \le t \le t_4 \\ a_4 + b_4 t + c_4 t^2 + d_4 t^3 + e_4 t^4 & \text{if } t_4 \le t \le t_5 \\ a_5 + b_5 t + c_5 t^2 + d_5 t^3 + e_5 t^4 & \text{if } t_5 \le t \le t_6, \end{cases} \quad (15)$$

where the subscript T denotes a six-tuple of time parameters, $T = (t_1, \ldots, t_6)$. There are 21 parameters, a_i, b_i, c_i d_i, e_i $(i = 1, 2, 4, 5)$ and the maximum bending angle A_m, in the definition of h. We impose 14 constraints, 8 of which are that the first and second derivatives at $t = t_1, t_3, t_4, t_6$ equal zero, and the remaining six are that the first to third derivatives at points t_2, t_5 are continuous. Therefore, the above parameters are uniquely determined for given time parameters $t_1, \ldots, t_6$ and the maximum bending angle A_m. An example of the trajectory h_T for a certain T is illustrated in Fig. 4.

3.2. *Optimization method for reference trajectory*

As stated in the preceding subsection, the reference trajectory h_T for a swing-leg knee angle is uniquely and completely determined when time parameters $t_1 \sim t_6$ and the maximum bending angle A_m are given. Since the dynamic equation of our model is nonlinear, a steady gait for the given reference trajectory is in general difficult to obtain analytically. In particular, our biped robot has 3 degrees of freedom, but has only one actuator at the swing-leg knee and, hence, the stance at heel strike cannot be determined *a priori*. Therefore, generating a steady gait is to rely on numerical simulation, which starts from a certain initial condition and succeeds to obtain a convergent steady gait by solving the dynamic equation and impact equation numerically. However, the initial condition itself strongly depends on the reference trajectory, and is difficult to determine *a priori*. Moreover, it takes a long simulation time to obtain a convergent steady gait from an initial condition. These issues are a significant drawback in optimizing a reference trajectory.

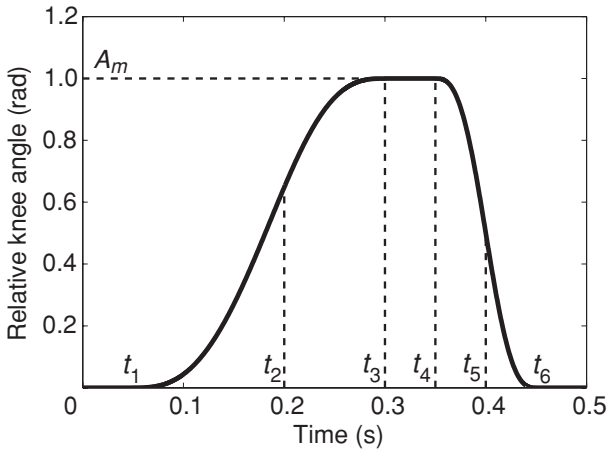

Fig. 4. Example of the reference trajectory using quartic spline curve.

Therefore, the optimization method proposed in this paper adopts the following strategy. The method starts from a steady gait corresponding to the reference trajectory known to generate sustainable walking and evaluate a walking performance index value for the steady gait. Next, the method perturbs slightly the above-mentioned reference trajectory and generates the steady gait corresponding to the perturbed trajectory from the above-mentioned gait as initial gait. When the difference between these trajectories is small enough, the difference between these corresponding steady gaits is also small, and it is expected to take a little time to generate a convergent steady gait. Then, if the walking performance index value of the perturbed trajectory is better than that of the original trajectory, we update the trajectory and the corresponding gait, and repeat the above procedure.

The generic optimization method for the given maximum bending angle A_m is summarized as follows.

Step 0 (Initialization). Choose a known steady gait W_0 corresponding to the reference trajectory h_{T_0} with six-tuple of time parameters $T_0 = (t_1^0, \ldots, t_6^0)$. Evaluate a walking performance index value p_0 for the gait W_0. Set $k = 0$.

Step 1. Choose $\bar{T}_k$ from a neighborhood of T_k.

Step 2. Starting from the gait W_k, perform a simulation until the gait converges to the steady gait $\bar{W}_k$ corresponding to the reference trajectory $h_{\bar{T}_k}$.

Step 3. If the simulation fails to converge, or if the walking performance index value $\bar{p}_k$ for the gait $\bar{W}_k$ is worse than p_k, choose another $\bar{T}_k$ and repeat Step 2. If there is no candidate of $\bar{T}_k$ in a neighborhood of T_k, stop. Output the current gait W_k.

Step 4 (Update). Set $W_{k+1} = \bar{W}_k$, $T_{k+1} = \bar{T}_k$, and $p_{k+1} = \bar{p}_k$. Set $k = k + 1$ and go to Step 1.

It is worth mentioning some practical implementation issues. The first and significant issue is that the search space for time parameters $t_1 \sim t_6$ is inherently continuous. However, numerical simulation is in general implemented in discrete time spaces on a computer and, hence, we discretize the search space *a priori*. According to this, we adopt the neighborhood of T_k in Steps 1 and 3, as the Hamming distance between $\bar{T}_k$ and T_k is one, that is, one of time parameters $t_1 \sim t_6$ is different with one unit.

The second issue is a walking performance index which is an object of the above optimization algorithm. In the numerical simulations in the next section, we use the four indices, namely the average walking speed, the foot clearance which is the highest position of the bottom of a swing

https://doi.org/10.1017/S0263574710000342 Published online by Cambridge University Press

leg, the maximum value of input torque, and the specific resistance (SR). Among them, the SR, which represents energy efficiency,[8] is defined as

$$\mathrm{SR} = \frac{\int_{0^+}^{T^-} |u_K(\dot{\theta}_2 - \dot{\theta}_3)|\mathrm{d}t/T}{M_g g \overline{V}}. \tag{16}$$

In Eq. (16), 0^+ and T^- represent the time just after and before the collision, respectively, at the ground, M_g is the total mass of a biped robot, and $\overline{V}$ is the walking speed of one step. The smaller the SR value is, the more efficient a walking is.

The proposed algorithm is inherently the same as local search methods usually used in combinatorial optimization problems and, hence, the method in general can find a local minimum only. In particular, the local minima obtained by the algorithm depend on an initial steady gait and the selection rule from a neighborhood in Steps 1 and 3.

4. Simulation Results

In this section, we show the simulation results of the optimization method proposed in the previous section applied for the biped model (Fig. 2), whose physical parameters are shown in Table I.

In the simulation, the time parameter t_6 is fixed as $t_6 = T_{set} = 0.45$ s, and the search space for the other time parameters $t_1, \ldots, t_5$ is the interval [0, 0.45], which is discretized in 0.01 s. The initial steady gait corresponds to the reference trajectory h defined by (15) with $A_m = 1.00$ rad, $t_1 = 0.14$, $t_2 = 0.19$, $t_3 = 0.30$, $t_4 = 0.30$, $t_5 = 0.44$, and $t_6 = 0.45$. The selection rule of a neighborhood in Steps 1 and 3 is $t_1, t_2, \ldots, t_5$ in order. In the simulation, when a local optimal solution is obtained, then the maximum bending angle A_m reduced by 0.01 rad, and the optimization method is applied again in which the previous local optimal gait is as the initial gait. This procedure is repeated until a steady gait is failed to be found.

For the comparison purpose, we also optimize the reference trajectory $\tilde{h}$ defined (12) using cubic sinusoid. In this case, T_{set} is fixed as $T_{set} = 0.45$ s and the optimal bending delay δ is found for each A_m by a simple exhaustive search for the interval [0, 0.45] discretized in 0.01.

4.1. Comparison between h and $\tilde{h}$

We first present the results of optimization with respect to SR. The results are summarized in Figs. 5 and 6. In these figures, circles denote the results for quartic spline curve h and crosses denote those for cubic sinusoid $\tilde{h}$. Figure 5 depicts the optimal SR for each bending angle A_m, and corresponding walking speed is depicted in Fig. 6. From Fig. 5, it is observed that the reference trajectory h using quartic spline curves is more efficient than $\tilde{h}$ using cubic sinusoid. In addition, the reference trajectory h can generate a sustainable gait in the region $A_m \geq 0.63$ rad, while the reference trajectory $\tilde{h}$ can generate the gait in the region $A_m \geq 0.76$ rad. This result suggests that the reference trajectory h can restore more energy than the reference trajectory $\tilde{h}$ at small A_m. It is observed from Fig. 5 that there is an optimal bending angle with respect to SR, such as about 0.71 rad for the reference trajectory h and about 0.82 rad for $\tilde{h}$, while in both cases walking speed is faster as bending angle becomes larger as shown in Fig. 6.

Table I. Physical parameters of the robot.

a_2	0.18	m	R	0.15	m
a_1	0.12	m	m_1	0.4	kg
r_2	0.09	m	m_2	1.6	kg
r_1	0.06	m	m_H	2.2	kg
l	0.30	m			

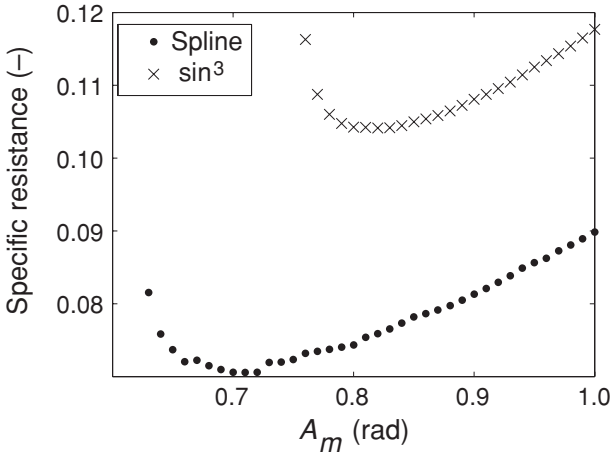

Fig. 5. Comparison of SR between h and $\tilde{h}$.

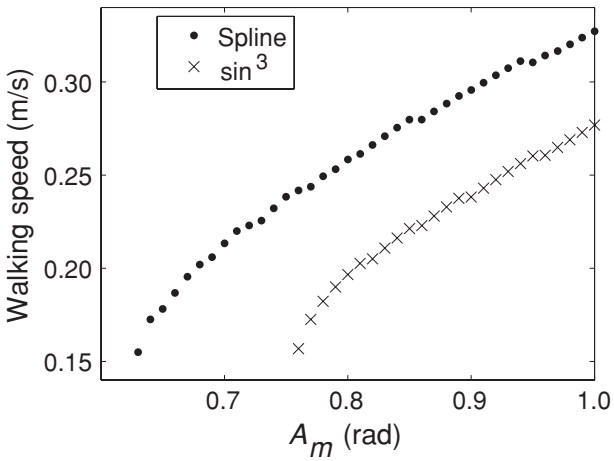

Fig. 6. Comparison of walking speeds between h and $\tilde{h}$.

To see in more detail, we consider the case of the maximum bending angle $A_m = 0.82$ rad, which is the most efficient in $\tilde{h}$. Table II shows the value of four walking performance indices, such as SR, walking speed, the maximum torque, and foot clearance, for the optimal trajectories h and $\tilde{h}$ with $A_m = 0.82$ rad. From Table II, the walking speed and the foot clearance of the reference trajectory h are larger than those of $\tilde{h}$, while the maximum torque of the reference trajectory $\tilde{h}$ is smaller than that of h. Figure 7 illustrates the optimal trajectories for h and $\tilde{h}$. In Fig. 7, the solid line denotes h and the dashed line denotes $\tilde{h}$. Time parameters of the trajectory with h are shown in Table III, and the optimal delay δ for $\tilde{h}$

https://doi.org/10.1017/S0263574710000342 Published online by Cambridge University Press

Table II. Simulation results.

	$\tilde{h}$	h
SR [−]	0.1041	0.0759
Walking speed (m/s)	0.2050	0.2662
Maximum torque (Nm)	0.6440	0.7518
Foot clearance (mm)	0.075	0.338

Table III. Optimal parameters.

t_1	t_2	t_3	t_4	t_5	t_6
0.17	0.22	0.29	0.34	0.44	0.45

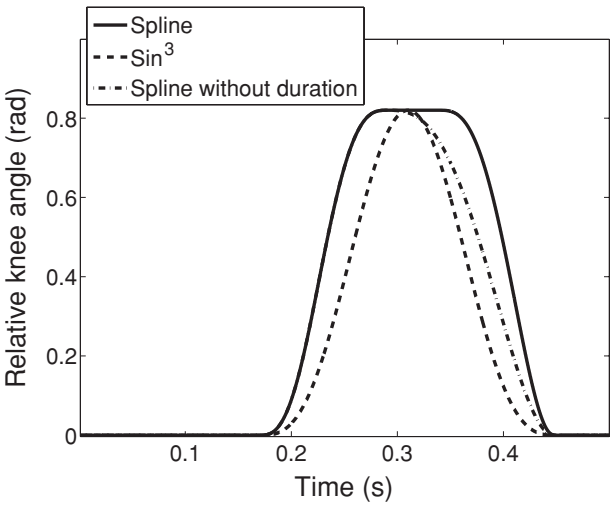

Fig. 7. Optimal trajectory for $A_m = 0.82$ rad.

is 0.18 s. It is observed from Fig. 7 that the swing-leg knee is kept in the maximum bending angle about 0.05 s in h. This is one reason why the reference trajectory h is more efficient than $\tilde{h}$.

Next, we present the results of optimizing the trajectory h with $A_m = 0.82$ rad in limiting the duration, $(t_4 - t_3)$ of keeping the maximum bending angle, to show the effect of duration. Table IV shows the optimal SR, walking speed (denoted by WS), and time parameters. From the table, it is observed that SR is larger, and walking speed is smaller as max $(t_4 - t_3)$ is smaller. Table IV shows that the result of h without duration (that is, $(t_4 - t_3) = 0$) is more efficient than that of $\tilde{h}$ with the same maximum bending angle $A_m = 0.82$ rad. The trajectory of this case is also depicted in Fig. 7 (denoted by the dot-dashed line). By comparison of this with

Table V. Results of similar walking speed.

	$\tilde{h}$	h
A_m (rad)	0.97	0.82
SR (−)	0.1143	0.0759
Walking speed (m/s)	0.2648	0.2662
Maximum torque (Nm)	0.8191	0.7518
Foot clearance (mm)	0.386	0.338

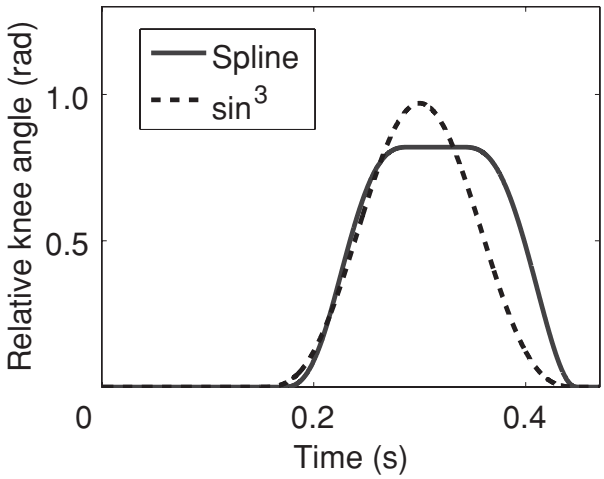

Fig. 8. Reference trajectory of the similar walking speed.

$\tilde{h}$, it is found that the efficiency of h more than $\tilde{h}$ is brought by the flexibility, in particular, asymmetricity, of h.

Next, we compare the optimal reference trajectories between h and $\tilde{h}$ with respect to SR in the case of almost same walking speed, about 0.265 m/s. The results are shown in Figs. 8 and 9 and Table V. Figure 8 shows the optimal reference trajectories, where the solid line denotes h and the dashed line denotes $\tilde{h}$. Figure 9(a) shows the angular position of the reference trajectory h, Fig. 9(b) shows the mechanical energy of the reference trajectory h, Fig. 9(c) shows the angular position of the reference trajectory $\tilde{h}$, and Fig. 9(d) shows mechanical energy of the reference trajectory $\tilde{h}$. From Figs. 9(b) and (d), it is observed that the variation of mechanical energy of the reference trajectory h is smaller than that of $\tilde{h}$. This is another certification that the reference trajectory h is more efficient than $\tilde{h}$. In general, the variation of mechanical energy equals input power and, hence, the smaller the variation of mechanical energy is, the more efficient a walking is in the case of almost the same walking speed. We note that from Figs. 9(b) and (d) the energy lost by the knee collision is almost zero for

Table IV. Optimal parameters subject to duration of keeping the maximum bending.

max$(t_4 - t_3)$	$SR\,(-)$	WS (m/s)	t_1	t_2	t_3	t_4	t_5	t_6
0.05	0.0759	0.2662	0.17	0.22	0.29	0.34	0.44	0.45
0.04	0.0768	0.2624	0.17	0.22	0.29	0.33	0.44	0.45
0.03	0.0786	0.2576	0.17	0.22	0.29	0.32	0.44	0.45
0.02	0.0808	0.2518	0.17	0.22	0.29	0.31	0.44	0.45
0.01	0.0835	0.2449	0.17	0.22	0.29	0.30	0.44	0.45
0.00	0.0870	0.2365	0.17	0.22	0.29	0.29	0.44	0.45

https://doi.org/10.1017/S0263574710000342 Published online by Cambridge University Press

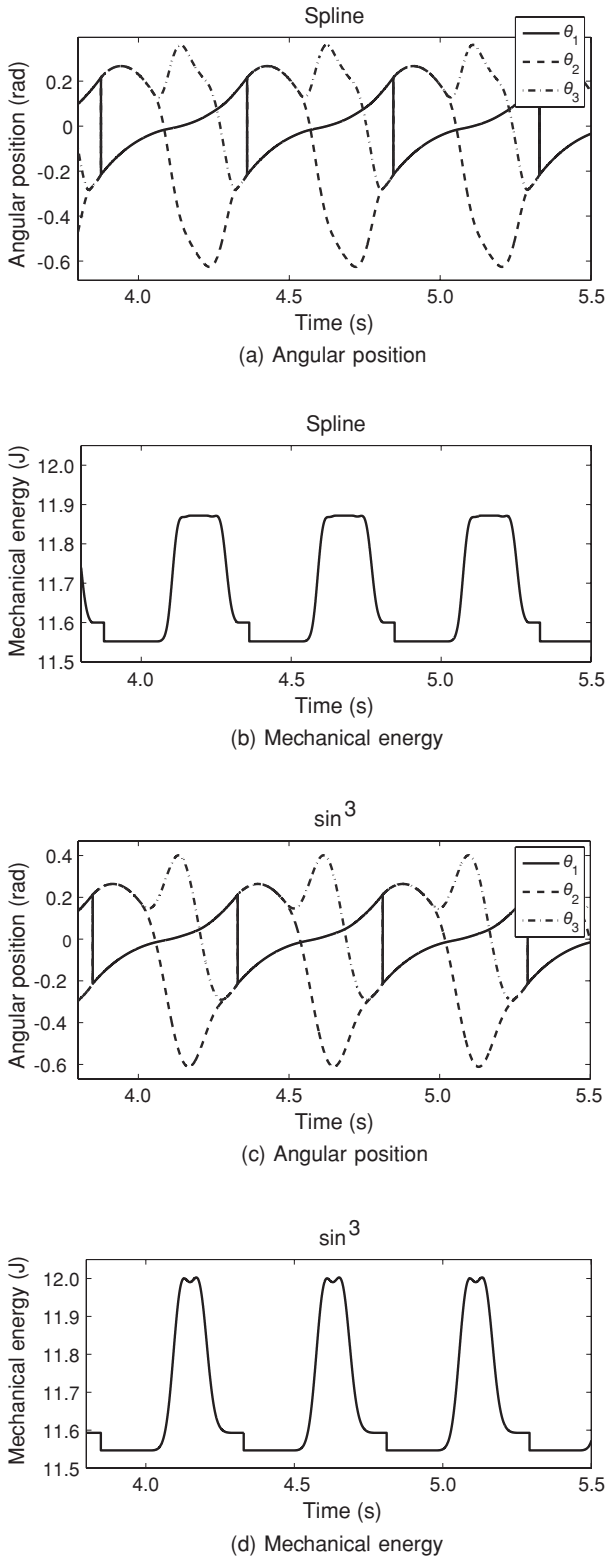

Fig. 9. Simulation results of same walking speed.

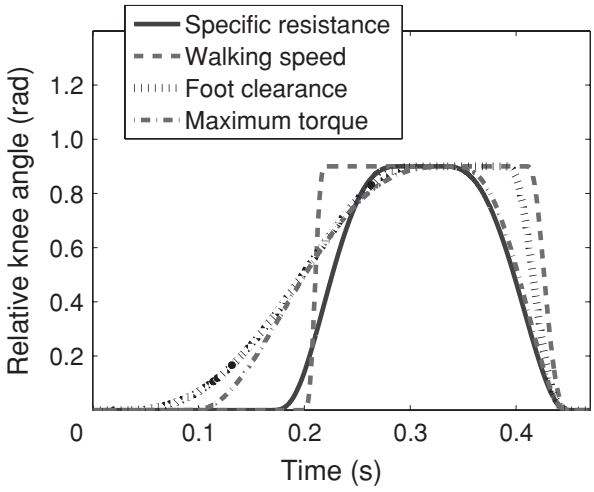

Fig. 10. Optimal trajectories for each index.

both reference trajectories h and $\tilde{h}$. Table V summarizes the maximum bending angle and walking performance index values for the gaits shown in Fig. 9. From the table, it is observed that the SR and the maximum input torque of the reference trajectory h are better than those of $\tilde{h}$, while the foot clearance of h is worse than that of $\tilde{h}$. This is simply because that the maximum bending angle A_m of $\tilde{h}$ is larger than that of h.

Simulation results in this section show that the reference trajectory h is more efficient than $\tilde{h}$. This is because of the duration of keeping the maximum bending angle and asymmetricity of h. In addition, it is observed from Table II that the foot clearance of the reference trajectory h is larger than that of the reference trajectory $\tilde{h}$. This is because the end of bending swing leg of h is faster than that of $\tilde{h}$.

4.2. Results with respect to other walking performance indices

Finally, we present the results of optimization with respect to other indices, such as walking speed, foot clearance, and the maximum input torque. In the simulations, we fix the maximum bending angle and the time parameter t_6 as $A_m = 0.90$ rad and $t_6 = 0.45$ s, respectively.

The results are summarized in Tables VI and VII and Fig. 10. Table VI presents performance index values. The first row of Table VI presents the results with respect to walking speed, the second row presents those with respect to foot clearance, the third row presents those with respect to the maximum input torque and the forth row presents those with respect to the SR. Figure 10 illustrates the optimal trajectories for each performance index and the corresponding time parameters are shown in Table VII. In Fig. 10, the solid

Table VI. Results of optimization with respect to some indices.

Index	WS (m/s)	FC (mm)	MT (Nm)	SR (−)
Walking speed (WS)	0.3350	0.409	39.1941	1.2922
Foot clearance (FC)	0.2396	1.504	4.4147	0.2664
Maximum torque (MT)	0.2758	0.758	0.7071	0.0942
Specific resistance (SR)	0.2957	0.488	0.8391	0.0813

https://doi.org/10.1017/S0263574710000342 Published online by Cambridge University Press

Table VII. Parameters of optimal trajectories.

Index	t_1	t_2	t_3	t_4	t_5	t_6
Walking speed	0.20	0.21	0.22	0.41	0.42	0.45
Foot clearance	0.02	0.27	0.31	0.39	0.41	0.45
Maximum torque	0.09	0.12	0.34	0.34	0.44	0.45
SR	0.17	0.20	0.29	0.33	0.44	0.45

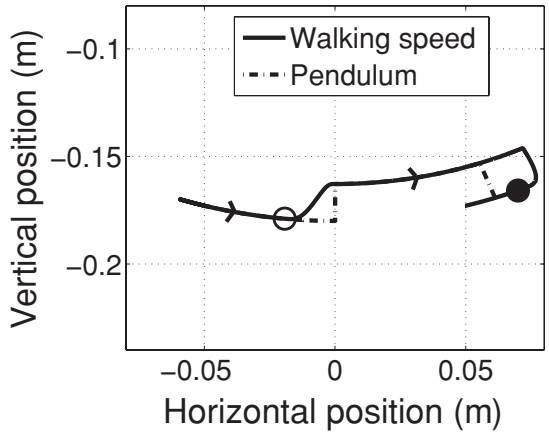

Fig. 11. Position of CoM of swing leg.

line denotes the optimal trajectory for SR, the dashed line denotes the optimal trajectory for walking speed, the dotted line denotes the optimal trajectory for foot clearance, and the dot-dashed line denotes the optimal trajectory for maximum torque.

From Table VI, it is observed that maximum torque is large in the case of foot clearance and walking speed. In particular, the optimized result for walking speed needs the maximum input torque, 39 Nm, and hence, SR is the largest. This is because the knee motion in this case is very quick, such as the interval of bending is 0.02 s. From Fig. 10 and Table VII, it is observed that the beginning of the bending, t_1, is early in the case of optimizing foot clearance. In the case of optimizing maximum torque, there is no keeping interval. The obtained trajectory for walking speed seems impossible to be realized with a real actuator because it requires too large torque, about 39 Nm. In the case of foot clearance, knee torque is relatively large compared with a robot size and, hence, it also seems difficult to realize the trajectories with a real actuator. On the other hand, the obtained trajectories for maximum torque and SR may be realized with a real actuator in view of maximum torque.

We remark that the optimal trajectory with respect to walking speed is very close to the optimal trajectory for the pendulum shown in Fig. 1. To see this in more detail, we depict the relative position of CoM of swing leg in one step. In Fig. 11, the solid line denotes the optimal trajectory of CoM of swing leg with respect to walking speed, and the dot-dashed line denotes the optimal trajectory for pendulum, the direction of the motions is indicated by arrows, the origin is corresponding to the position of hip joint of the robot, the horizontal axis represents horizontal position and the vertical axis represents vertical position. The white circle denotes the position of the beginning of bending and the black circle denotes the position of the end of stretching of the optimal trajectory of CoM of the swing leg with respect to walking speed. From Fig. 11, it is observed in the optimal trajectory with respect to walking speed that CoM is raised very quickly at the bottom of the swing leg and it was also made down very quickly at the highest point. This indicates that the trajectory of CoM of the swing leg is very close to the optimal trajectory for the pendulum. This is a remarkable result which reveals that the optimal trajectory for the pendulum is also meaningful for parametric excitation walking in a certain sense, despite that the structure of the pendulum and a biped robot are quite different.

There is no keeping interval in the case of optimizing maximum torque. The faster the knee motion is, the larger torque is required. Hence, the reference trajectory has no keeping interval in order to smooth the knee motion. When maximum torque is small, walking speed is small. On the other hand, when walking speed is large, large torque is required. Therefore, the reference trajectory in the case of optimizing SR is between that of walking speed and maximum torque in some sense. To increase foot clearance, a biped robot should keep bending swing leg. As a result of the optimization for foot clearance, the beginning time of bending swing leg becomes early and the end of stretching swing leg delays.

Remark 4.1. *We set the maximum step for solving differential equation numerically with MATLAB as* 0.001 *s and, hence, we chose discretization for the trajectory time as* 0.01 *s (10 times larger than maximum integral step). If we discretize the trajectory time finer, we should make maximum integral step finer. However, small integral time causes large time consumption and may cause numerical error. Therefore, we chose discretization for the trajectory time as* 0.01 *s.*

All simulations were implemented on WINDOWS XP SP3, Core 2 Duo 3.16 GHz, 3.25 GB memory with MATLAB R2008a. It takes about 360 *s on average to converge a steady gait and to evaluate a walking performance index value after each perturbation.*

5. Conclusion and Future Works

In this paper, we proposed the optimization method for parametric excitation walking. We utilized the quartic spline curve instead of cubic sinusoid and optimized the parameters of spline curve with respect to some indices. Simulation results showed that the proposed method could yield various gaits corresponding to maximum walking speed, maximum foot clearance, minimum input torque, and the most energy efficiency. For example, the SR of optimal gait was three-tenths of previous parametric excitation walking. In addition,

https://doi.org/10.1017/S0263574710000342 Published online by Cambridge University Press

we showed that the optimal trajectory with respect to walking speed is very close to the optimal trajectory for the pendulum.

Some remarks and subjects of future works are summarized as follows.

(1) The proposed method in general could find a local minimum only. We expect that the proposed method will be improved by incorporating with some globalizing technique, such as genetic algorithm (GA), multi-start local search, and so on.
(2) In this paper, we use a quartic spline curve to make the acceleration smooth. When the obtained trajectories are applied to a real robot, an actuator will be controlled by proportional-derivative (PD) controller and, hence, a knee may not track the reference trajectory completely. On the other hand, some modifications of the proposed method are available soon, such that, introducing five-order spline curves to smooth jerk, or introducing a maximum torque constraint. To clarify how much these modifications influence the results is also one of the subjects for future research.
(3) The proposed method optimized the reference trajectory only. To grow in more efficiency, it is important to optimize the physical parameters of the biped robot, for example mass and link length.
(4) Another method to grow in efficiency is the parametric excitation based ornithoid walking[4,5] and the combined parametric excitation walking proposed by Harata *et al.*[9] In the next paper, we will apply the proposed optimization method to the above parametric excitation walking methods and will improve the efficiency of these methods.

References

1. F. Asano, Z. W. Luo and S. Hyon, "Parametric Excitation Mechanisms for Dynamic Bipedal Walking," *Proceedings of the IEEE International Conference on Robotics and Automation* (2005) pp. 611–617.
2. Y. Harata, F. Asano, Z. W. Luo, K. Taji and Y. Uno, "Biped Gait Generation Based on Parametric Excitation by Knee-joint Actuation," *Proceedings of the IEEE/RSJ International Conference on Intelligent Robots and Systems* (2007) pp. 2198–2203.
3. Y. Harata, F. Asano, Z. W. Luo, K. Taji and Y. Uno, "Biped gait generation based on parametric excitation by knee-joint actuation," *Robotica* **27**, 1063–1073 (2009).
4. Y. Harata, F. Asano, K. Taji and Y. Uno, "Parametric Excitation Based Gait Generation for Ornithoid Walking," *Proceedings of the IEEE/RSJ International Conference on Intelligent Robots and Systems* (2008) pp. 2940–2945.
5. Y. Harata, F. Asano, K. Taji and Y. Uno, "Ornithoid gait generation based on parametric excitation," *J. Robot. Soc. Japan* **27**, 575–582 (2009) (in Japanese).
6. E. K. Lavrovskii and A. M. Formal'skii, "Optimal control of the pumping and damping of swing," *J. Appl. Math. Mech.* **57**(2), 311–320 (1993).
7. C. Chevallereau and Y. Aoustin, "Optimal reference trajectories for walking and running of a biped robot," *Robotica* **19**(5), 557–569 (2001).
8. G. Gabrielli and Th. von Karman, "What price speed? Specific power required for propulsion of vehicles," *Mech. Eng.* **72**(10), 775–781 (1950).
9. Y. Harata, F. Asano, K. Taji and Y. Uno, "Parametric Excitation Walking for Four-linked Bipedal Robot," *Preprints of the 9th IFAC Symposium on Robot Control* (2009) pp. 589–594.

https://doi.org/10.1017/S0263574710000342 Published online by Cambridge University Press